

Demonstration of Ground Vehicle Navigation with Non-cooperative Multi-constellation LEO Satellites

Samer Hayek, Joe Saroufim, Sharbel Kozhaya, Will Barrett, and Zaher M. Kassas
The Ohio State University

BIOGRAPHY

Samer Hayek is a Ph.D student in the Department of Electrical and Computer Engineering at The Ohio State University and a member of the Autonomous Systems Perception, Intelligence, and Navigation (ASPIN) Laboratory. He received a B.E. in Mechanical Engineering from the Lebanese American University. His current research interests include low Earth orbit satellites, autonomous vehicles, sensor fusion, and simultaneous localization and mapping.

Joe Saroufim is a Ph.D student in the Department of Electrical and Computer Engineering at The Ohio State University and a member of the ASPIN Laboratory. He received a B.E. in Mechanical Engineering from the Lebanese American University. His current research interests include low Earth orbit satellites, situational awareness, autonomous vehicles, and sensor fusion.

Sharbel Kozhaya is a Ph.D student in the Department of Electrical and Computer Engineering at The Ohio State University and a member of the ASPIN Laboratory. He received a B.E. in Electrical Engineering from the Lebanese American University. His current research interests include opportunistic navigation, low Earth orbit satellites, cognitive software-defined radio, and 5G. He is the recipient of the 2023 IEEE/ION Position, Location, and Navigation Symposium (PLANS) best student paper award.

Will Barrett is an M.S. student in the Department of Electrical and Computer Engineering at The Ohio State University and a member of the ASPIN Laboratory. He received a B.S. in Electrical and Computer Engineering from The Ohio State University. His current research interests include Satellite-based navigation and sensor fusion.

Zaher (Zak) M. Kassas is the TRC Endowed Chair in Intelligent Transportation Systems and a professor at The Ohio State University. He is the Director of the ASPIN Laboratory. He is also Director of the U.S. Department of Transportation Center: CARMEN (Center for Automated Vehicle Research with Multimodal AssurEd Navigation), focusing on navigation resiliency and security of highly automated transportation systems. He received a B.E. with Honors in Electrical Engineering from the Lebanese American University, an M.S. in Electrical and Computer Engineering from The Ohio State University, and an M.S.E. in Aerospace Engineering and a Ph.D. in Electrical and Computer Engineering from The University of Texas at Austin. He is a recipient of the National Science Foundation (NSF) CAREER award, Office of Naval Research (ONR) Young Investigator Program (YIP) award, Air Force Office of Scientific Research (AFOSR) YIP award, IEEE Walter Fried Award, IEEE Harry Rowe Mimno Award, Institute of Navigation (ION) Samuel Burka Award, and ION Col. Thomas Thurlow Award. He is a Fellow of the IEEE, a Fellow of the ION, and a Distinguished Lecturer of the IEEE Aerospace and Electronic Systems Society and the IEEE Intelligent Transportation Systems Society. His research interests include cyber-physical systems, navigation systems, low Earth orbit satellites, cognitive sensing, and intelligent transportation systems.

ABSTRACT

An experimental demonstration of a ground vehicle navigating exclusively with non-cooperative multi-constellation low Earth orbit (LEO) satellite signals of opportunity is presented. The satellites' unknown downlink signals are processed through a cognitive software-defined receiver to extract Doppler frequency measurements. To account for the satellites' uncertain timing and ephemerides, a correction approach is employed in a standalone fashion (i.e., by the vehicle-mounted receiver) during an initial period of global navigation satellite system (GNSS) signal availability. The approach accounts for ephemerides reference time errors and large orbit errors that are inherited from simplified general perturbation 4 (SGP4) open-loop propagation of publicly available two-line element (TLE) files. Results are presented showcasing the ground vehicle navigating by fusing via an extended Kalman filter (EKF) Doppler measurements from 4 Starlink, 1 OneWeb, 2 Orbcomm, and 1 Iridium NEXT LEO satellites. The vehicle traversed a total trajectory of 1.58 km in 70 seconds, during which GNSS signals were unavailable for the final 1.054 km, corresponding to a 40-second duration. Without GNSS, the unaided navigation solution resulted in a three-dimensional (3D) root mean squared error (RMSE) of 110 m. In contrast, navigating with LEO signals of opportunity achieved an RMSE of 4.15 m, which is an unprecedented level of accuracy with non-cooperative LEO.

I. INTRODUCTION

Low Earth orbit (LEO)-based communication has been offered over the past couple of decades by constellations; such as Orbcomm, Iridium, and Globalstar; each of which composed of *tens* of LEO space vehicles (SVs). However, the launch of LEO megaconstellations; such as Starlink, OneWeb, Kuiper, Telesat, and SpaceMobile; which are aggregate planning to launch *tens of thousands* of LEO SVs is promising to revolutionize several domains, bringing unprecedented high-resolution images; remote sensing; and global, high-availability, high-bandwidth, and low-latency Internet (Osoro and Oughton, 2021). These LEO satellite megaconstellations are expected to shape a new era of satellite-based navigation.

LEO megaconstellations inherently possess desirable attributes for positioning, navigation, and timing (PNT) (Stock et al., 2024): (i) geometric and spectral diversity, (ii) abundance, (iii) high received signal power, and (iv) high orbital velocity. As such, LEO satellites could offer an attractive complement or even an alternative to global navigation satellite systems (GNSS), which reside in medium Earth orbit (MEO) (Reid et al., 2021; Kassas, 2021; Prol et al., 2022; Jardak and Jault, 2022). The promise of utilizing LEO SVs for navigation has been the subject of numerous recent theoretical (Wei et al., 2020; Thompson et al., 2020; Psiaki, 2021; Hartnett, 2022; Cassel et al., 2022; Jiang et al., 2022; Khalife and Kassas, 2023; Sabbagh and Kassas, 2023; Kang et al., 2024) and experimental (Leng et al., 2016; Tan et al., 2019a; Farhangian and Landry, 2020; Farhangian et al., 2021; Wang and El-Mowafy, 2022; Huang et al., 2022; Li et al., 2022; Kassas et al., 2023) studies. While some of these studies proposed to design LEO satellite constellations dedicated for navigation (Reid et al., 2020; Nardin et al., 2021; Ries et al., 2023; Menziane and Paonni, 2023; Yan et al., 2023) other studies proposed to exploit LEO satellite signals of opportunity for PNT purposes (Tan et al., 2019b; Zhao et al., 2022; Shahcheraghi and Kassas, 2024; Xie et al., 2024).

Several challenges need to be addressed before LEO SV signals of opportunity could be used for PNT. First, there are no publicly available receivers that can produce navigation observables from LEO satellite signals. Recent papers have addressed this challenge for some of the existing constellations (Landry et al., 2019; Khalife and Kassas, 2019; Orabi et al., 2021; Huang et al., 2022; Khalife et al., 2022; Neinavaie et al., 2022; Kozhaya and Kassas, 2023; Kozhaya et al., 2023). Second, the ephemerides of LEO satellites are not as precisely known as those of GNSS satellites. Estimates of the Keplerian elements parameterizing the orbits of LEO satellites are made publicly available by the North American Aerospace Defense Command (NORAD) and are updated daily in the two-line element (TLE) files (Kelso, 2022). Using TLEs and orbit propagation algorithms (e.g., simplified general perturbation 4 SGP4 (Vallado and Crawford, 2008)), the positions and velocities of these satellites can be obtained, albeit not precisely (Vetter, 2007). Orbit propagation through SGP4 has been shown to exhibit errors concentrated along the SV's direction of motion (Kelso, 2007). Specifically, it was found that SGP4 propagation induces a linearly increasing error in the SV's argument of latitude orbital element (Easthope, 2015). Third, LEO SVs' clock errors and oscillator stability are generally unknown.

Previous research addressed the last two challenges by developing the simultaneous tracking and navigation (STAN) framework (Kassas et al., 2024), where LEO observables aid the inertial navigation system (INS) of a navigating vehicle, while simultaneously estimating the position, velocity, and clock states of LEO satellites. Recently, the incorporation of LEO observables from a cooperative reference base-station was shown to substantially improve the navigation accuracy of LEO-PNT systems (Khalife and Kassas, 2023; Saroufim et al., 2023; Zhao et al., 2023). Ground vehicle navigation has been demonstrated experimentally with the STAN (Kassas et al., 2024) and differential STAN (Saroufim et al., 2024) frameworks.

An alternative framework to STAN and differential was proposed in (Hayek et al., 2023, 2024b), which relies on recursive estimation of the argument-of-latitude to mitigate the large ephemeris errors inherited from TLE-initialized SGP4 orbit propagation. Moreover, (Hayek and Kassas, 2024) studied the effect of timing and spatial ephemeris errors on navigation observables extracted from non-cooperative LEO satellite signals, developing a batch estimation approach to resolve those errors in a short period of time during which GNSS signals are available. This paper experimentally demonstrates this ephemeris error correction approach on a ground vehicle navigating by fusing via an extended Kalman filter (EKF) Doppler frequency measurements from multi-constellation LEO SVs, namely, 4 Starlink, 1 OneWeb, 2 Orbcomm, and 1 Iridium NEXT SVs. The vehicle traversed a total trajectory of 1.58 km in 70 seconds, during which GNSS signals were unavailable for the final 1.054 km, corresponding to a 40-second duration. Without GNSS, the unaided navigation solution resulted in a three-dimensional (3D) root mean squared error (RMSE) of 110 m. In contrast, navigating with LEO signals of opportunity achieved an RMSE of 4.15 m, which is an unprecedented level of accuracy with non-cooperative LEO.

The rest of the paper is organized as follows. Section II describes the vehicle dynamics model, clock error dynamics model, measurement model, and EKF navigation framework formulation. Section III presents the experimental results. Section IV gives concluding remarks.

II. MODEL DESCRIPTION

This section presents the vehicle and clock error dynamics, the Doppler frequency measurement model, and the EKF navigation framework formulation.

1. Vehicle Dynamics

The vehicle dynamics will assume a simple, yet reasonable, dynamical model: velocity random walk, which can be expressed as (Li and Jilkov, 2003)

$$\mathbf{x}_{\text{pv}}(k+1) = \mathbf{F}_{\text{pv}}\mathbf{x}_{\text{pv}}(k) + \mathbf{w}_{\text{pv}}(k), \quad (1)$$

where $\mathbf{x}_{\text{pv}} \triangleq [\mathbf{r}_r^\top, \dot{\mathbf{r}}_r^\top]^\top$ consists of the 3D position and velocity vectors of the vehicle, resolved in the Earth-centered Earth-fixed (ECEF) reference frame, $\mathbf{F}_{\text{pv}} \triangleq \begin{bmatrix} \mathbf{I}_{3 \times 3} & T\mathbf{I}_{3 \times 3} \\ \mathbf{0}_{3 \times 3} & \mathbf{I}_{3 \times 3} \end{bmatrix}$ is the state transition matrix, $\mathbf{I}_{n \times n}$ is the $n \times n$ identity matrix, $\mathbf{0}_{n \times n}$ is the $n \times n$ zero matrix, T is the sampling interval, and \mathbf{w}_{pv} is the process noise, which is modeled as a zero-mean, white random vector with covariance \mathbf{Q}_{pv} that can be readily obtained from the acceleration process noise power spectra (Kassas and Humphreys, 2014).

2. Clock Dynamics

The clock error state vector \mathbf{x}_{clk} will be composed of the bias δt and drift $\dot{\delta t}$, i.e., $\mathbf{x}_{\text{clk}} \triangleq [\delta t, \dot{\delta t}]^\top$. The dynamics of \mathbf{x}_{clk} is modeled to evolve according to a double integrator, driven by process noise (Brown and Hwang, 2012), according to

$$\mathbf{x}_{\text{clk}}(k+1) = \mathbf{F}_{\text{clk}}\mathbf{x}_{\text{clk}}(k) + \mathbf{w}_{\text{clk}}(k), \quad (2)$$

where $\mathbf{F}_{\text{clk}} \triangleq \begin{bmatrix} \mathbf{I}_{3 \times 3} & T\mathbf{I}_{3 \times 3} \\ \mathbf{0}_{3 \times 3} & \mathbf{I}_{3 \times 3} \end{bmatrix}$ and \mathbf{w}_{clk} is the process noise, which is modeled as a zero-mean, white random vector with covariance \mathbf{Q}_{clk} that can be readily obtained from the power spectral densities (PSDs) corresponding to the oscillator quality (Kassas and Humphreys, 2014). Since \mathbf{x}_{clk} will be defined as the difference between the receiver's and LEO SV's clock error states, then its dynamics will be similar to (2) except that its process noise covariance will be written in terms of the two process noise covariances, $\mathbf{Q}_{\text{clk},r}$ and $\mathbf{Q}_{\text{clk},s}$ (Kassas et al., 2024).

3. Doppler Frequency Measurement Model

Previous literature has demonstrated receiver structures that are able to extract Doppler frequency observables from multi-constellation LEO SV signals (Kozhaya et al., 2023). The Doppler measurement f_D extracted by the LEO receiver is related to the pseudorange rate measurement $\dot{\rho}$ according to

$$\dot{\rho} = -\frac{c}{f_c} f_D, \quad (3)$$

where f_c is the LEO SV downlink signal carrier frequency and c is the speed-of-light. The pseudorange rate measurement is modeled as

$$\dot{\rho}(k) = [\dot{\mathbf{r}}_r(k) - \dot{\mathbf{r}}_s(k')]^\top \frac{\mathbf{r}_r(k) - \mathbf{r}_s(k')}{\|\mathbf{r}_r(k) - \mathbf{r}_s(k')\|_2} + c \cdot [\dot{\delta t}_r(k) - \dot{\delta t}_s(k')] + c\dot{\delta t}_{\text{ion}}(k) + c\dot{\delta t}_{\text{tro}}(k) + v_{\dot{\rho}}(k), \quad (4)$$

where \mathbf{r}_s and $\dot{\mathbf{r}}_s$ are the 3D position and velocity vectors of the LEO SV, resolved in the ECEF reference frame; k' represents discrete-time at $t_{k'} = t_k - \delta_{\text{TOF}}$, with δ_{TOF} being the true time-of-flight (TOF) of the signal from the LEO SV to the receiver; $\dot{\delta t}_{\text{ion}}$ and $\dot{\delta t}_{\text{tro}}$ are the ionospheric and tropospheric delay rates (drifts), respectively; and $v_{\dot{\rho}}$ is the pseudorange rate measurement noise, which is modeled as a discrete-time zero-mean white Gaussian sequence with standard deviation $\sigma_{\dot{\rho}}$.

4. Framework Formulation

The navigator implements the ephemerides timing and spatial error correction strategy developed in (Hayek and Kassas, 2024). Publicly available TLE files of the considered LEO SVs are propagated using the SGP4 orbit propagator to generate the predicted orbits, $\{\mathbf{r}'_{s,i}(t), \dot{\mathbf{r}}'_{s,i}(t)\}_{i=1}^L$, where i represents the LEO SV index and L is the total number of LEO SVs. A batch least-squares is employed to estimate each SV's argument of latitude error which accounts for the ephemeris reference time and along-track errors of each LEO SV. An epoch time adjustment is calculated from the argument of latitude as $\tau_i = \frac{r_{s,i}^2}{h_i} \tilde{u}_i$, where $r_s \triangleq \|\mathbf{r}_s\|_2$ and $h \triangleq \|\mathbf{r}_s \times \dot{\mathbf{r}}_s\|_2$ is the angular momentum vector magnitude. Consequently, the corrected ephemerides sets are generated as $\{\mathbf{r}'_{s,i}(t + \tau_i), \dot{\mathbf{r}}'_{s,i}(t + \tau_i)\}_{i=1}^L$ (Hayek et al., 2024a).

A block diagram of the framework is illustrated in Figure 1, where the discussed vehicle dynamics, clock models, and ephemeris error correction strategy are incorporated in an EKF that estimates the state vector

$$\mathbf{x} = [\mathbf{x}_{\text{pv}}^\top, \mathbf{x}_{\text{clk},1}^\top, \dots, \mathbf{x}_{\text{clk},L}^\top]. \quad (5)$$

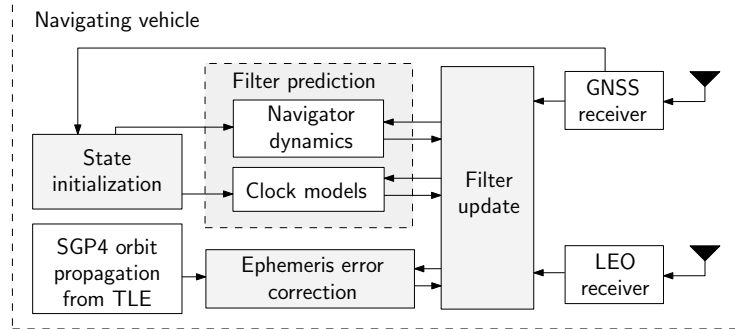


Figure 1: LEO-aided navigation with ephemeris error correction framework.

III. EXPERIMENTAL RESULTS

This section presents experimental results of a ground vehicle navigating with signals from multi-constellation LEO SVs via the framework discussed in Section II.4.

1. Experimental Setup

To demonstrate the framework described in Section II.4, a ground vehicle was equipped with a high-end VHF antenna to record Orbcomm signals, an L-band antenna to record Iridium NEXT signals, and a Ku-band low-noise block downconverter to record Starlink and OneWeb signals. The vehicle was equipped with universal software radio peripherals (USRs) to process and record the signals, where two Ettus B205mini's were used for the Orbcomm and Iridium signals while an NI-2954 was used for Starlink and OneWeb signals. The receivers' oscillators were all disciplined with a common GPS-disciplined oscillator. The receivers were tuned to the corresponding downlink signal carrier frequencies of each constellation: 137 MHz for Orbcomm, 1626 MHz for Iridium, and 10.825, 11.075, 11.325, and 11.575 GHz for Starlink and OneWeb. Samples of the received signals were stored for off-line post processing using the cognitive software-defined radios (SDRs) developed in (Kozhaya and Kassas, 2024; Kozhaya et al., 2024) to generate Doppler frequency measurements. All of the produced measurements were resampled to 100 Hz. The vehicle's ground truth trajectory was taken from the on-board GNSS-INS (inertial navigation system) Septentrio AsteRx SBi3 Pro+. The experimental hardware setup is shown in Figure 2. The vehicle traversed a total distance of 1.58 km in a duration of 70 seconds.

Over the course of the experiment, the receivers on-board the vehicle were listening to 2 Orbcomm SVs, 1 Iridium NEXT SV, 4 Starlink SVs, and 1 OneWeb SV. The generated Doppler measurements were converted to pseudorange rates (c.f. (3)), shown in Figure 3(a), to obtain comparable measurements from different constellations which transmit downlink signals at frequencies that are orders of magnitude apart. Figure 3(b) shows the measurement residuals obtained by differencing the predicted ranging (c.f. (4)) from the measured pseudorange rates, i.e., $\dot{p} = -\frac{c}{f_c} f_D$, for each LEO SV.

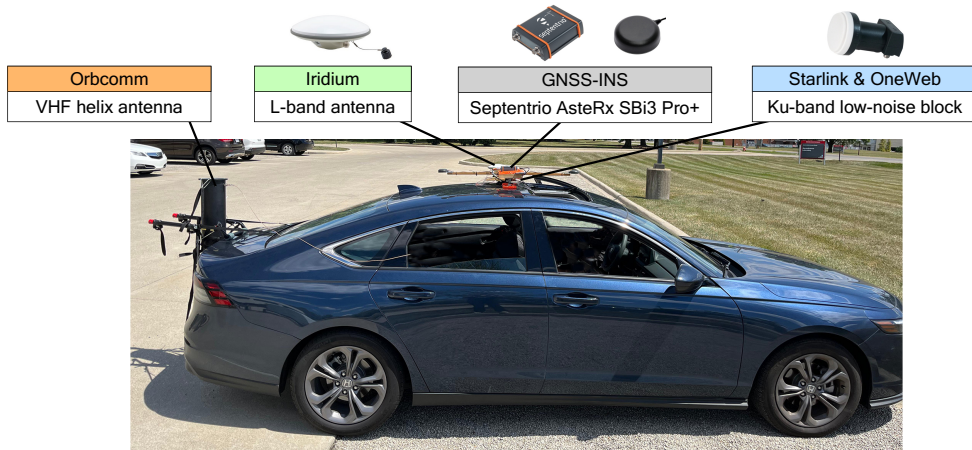


Figure 2: Ground vehicle hardware setup.

2. Navigation Filter Settings

The vehicle's continuous-time acceleration process noise spectra were set to $\tilde{q}_E = 0.6 \text{ m}^2/\text{s}^3$, $\tilde{q}_N = 0.2 \text{ m}^2/\text{s}^3$, and $\tilde{q}_U = 0.05 \text{ m}^2/\text{s}^3$ for the East, North, and Up (ENU) components, respectively. The choice of these spectra is due to the fact that the vehicle's dynamics are mainly in the horizontal direction. The vehicle's and LEO SV's oscillator qualities were both assumed to be that of a high-quality oven-controlled crystal oscillator (OCXO). A prior for the vehicle's position and velocity was obtained from the on-board GNSS-INS system. The initial vehicle ENU-frame position and velocity estimation error covariance values were set to $\mathbf{P}_{r_i}(0|0) \equiv \text{diag}[10, 10, 1] \text{ m}^2$ and $\mathbf{P}_{\dot{r}_i}(0|0) \equiv \text{diag}[1, 1, 0.1] \text{ (m/s)}^2$, respectively. The initial estimation error covariance for the relative clock error states of each SV was set to $\mathbf{P}_{\text{clk}}(0|0) \equiv \text{diag}[9 \times 10^4, 9 \times 10^2]$ with units $[\text{m}^2, \text{(m/s)}^2]$, corresponding to a 1σ of $1 \mu\text{s}$ and $0.1 \mu\text{s}/\text{s}$ for the clock bias and drift, respectively. The filter's time-varying pseudorange rate measurement noise standard deviations for the i -th LEO SV, $\sigma_{\dot{r}_i}(k)$, were set to be proportional to the measurement innovations for the Orbcomm and Iridium SVs and ranged between 0.0332 and 45.36 m/s and proportional to the square root of the inverse carrier-to-noise ratio (C/N_0), expressed in linear units (Kassas et al., 2024), for Starlink and OneWeb and ranged between 0.26 and 14.91 m/s . Altimeter measurements from the vehicle's on-board GNSS-INS navigation system were also fused into the EKF with a noise variance of 3 m^2 .

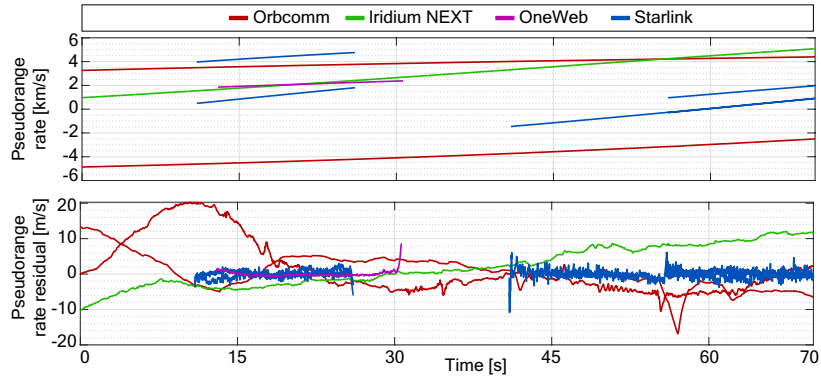


Figure 3: (a) Measured pseudorange rates (i.e., $-\frac{c}{f_c} f_D$) from multi-constellation LEO SVs and (b) their corresponding residuals with respect to the predicted range rates according to the vehicle and LEO SV dynamics.

3. Results

While the vehicle traversed a total trajectory of 1.58 km in 70 seconds , GNSS signals were made unavailable for the final 1.054 km , corresponding to a 40-second duration. Figure 4(top) shows the LEO SVs' trajectories with respect to the ground vehicle's location, while Figure 4(bottom) illustrates the ground truth trajectory traversed by the vehicle as well as the estimated vehicle trajectory without LEO-aiding versus the LEO-aided navigation solution. The unaided solution resulted in a 3D position RMSE of 110 m and diverged to a final error of 322 m . On the other hand, the LEO-aided solution, where the proposed framework described in Section II.4 was implemented, resulted in a 3D position RMSE of 4.15 m and a final error 8.13 m .

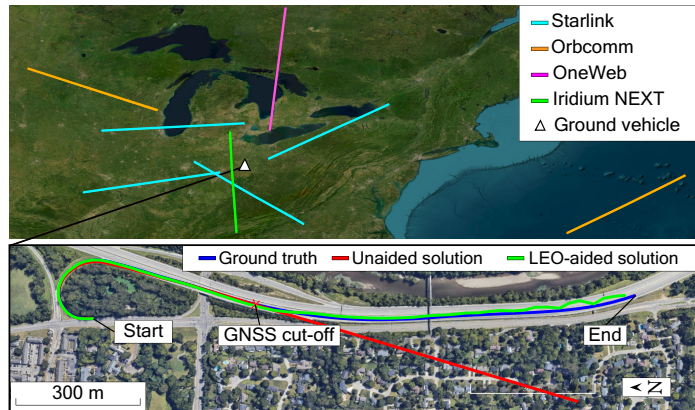


Figure 4: Experimental results: (Top) LEO SV trajectories of 4 Starlink, 1 OneWeb, 2 Orbcomm, and 1 Iridium LEO SV whose signals were exploited for ground vehicle navigation. (Bottom) vehicle's ground truth trajectory (blue), unaided solution (red), and LEO-aided solution (green). The vehicle traversed a trajectory of 1.58 km in 70 seconds , during which GNSS signals were unavailable for the final 1.054 km , corresponding to a 40-second duration. The unaided navigation solution's 3D position RMSE was 110 m , while the LEO-aided was 4.15 m .

Table 1: Experimental results: Ground vehicle 3D position RMSEs and final errors

	Position RMSE [m]	Final error [m]
Unaided Dynamics	110	322
LEO-aided dynamics	4.15	8.13

IV. CONCLUSION

This paper studied the incorporation of a LEO SV ephemeris error correction strategy for a dynamic navigator. The framework resolves the ephemeris reference time errors and large orbit errors that are inherited from TLE-initialized open-loop SGP4 orbit propagation. The approach was demonstrated experimentally with a ground vehicle navigating with Doppler frequency measurements from multi-constellation non-cooperative LEO SVs, namely, Starlink, Orbcomm, OneWeb, and Iridium NEXT. Over a trajectory of 1.58 km, the unaided navigation solution resulted in a vehicle 3D RMSE of 110 m, while the proposed LEO-aided approach achieved an RMSE of 4.15 m.

ACKNOWLEDGEMENTS

This work was supported in part by the Air Force Office of Scientific Research (AFOSR) under Grant FA9550-22-1-0476, by the Office of Naval Research (ONR) under Grants N00014-22-1-2242 and N00014-22-1-2115, by the National Science Foundation (NSF) under Grant 2240512, and by the U.S. Department of Transportation under Grant 69A3552348327 for the CARMEN+ University Transportation Center.

REFERENCES

Brown, R. and Hwang, P. (2012). *Introduction to Random Signals and Applied Kalman Filtering with Matlab Exercises*. John Wiley & Sons, fourth edition.

Cassel, R., Scherer, D., Wilburne, D., Hirschauer, J., and Burke, J. (2022). Impact of improved oscillator stability on LEO-based satellite navigation. In *Proceedings of ION International Technical Meeting*, pages 893–905.

Easthope, P. (2015). Examination of SGP4 along-track errors for initially circular orbits. *IMA Journal of Applied Mathematics*, 80(2):554–568.

Farhangian, F., Benzerrouk, H., and Landry, R. (2021). Opportunistic in-flight INS alignment using LEO satellites and a rotatory IMU platform. *Aerospace*, 8(10):280–281.

Farhangian, F. and Landry, R. (2020). Multi-constellation software-defined receiver for Doppler positioning with LEO satellites. *Sensors*, 20(20):5866–5883.

Hartnett, M. (2022). Performance assessment of navigation using carrier Doppler measurements from multiple LEO constellations. Master’s thesis, Air Force Institute of Technology, Ohio, USA.

Hayek, S. and Kassas, Z. (2024). Modeling and compensation of timing and spatial ephemeris errors of non-cooperative leo satellites with application to pnt. *IEEE Transactions on Aerospace and Electronic Systems*. submitted.

Hayek, S., Saroufim, J., and Kassas, Z. (2023). Ephemeris error modeling in opportunistic LEO satellite tracking with pseudorange and Doppler measurements. In *Proceedings of ION GNSS+ Conference*, pages 2123–2133.

Hayek, S., Saroufim, J., and Kassas, Z. (2024a). Analysis and correction of LEO satellite propagation errors with application to navigation. In *Proceedings of ION GNSS+ Conference*. accepted.

Hayek, S., Saroufim, J., and Kassas, Z. (2024b). Ephemeris error correction for tracking non-cooperative LEO satellites with pseudorange measurements. In *Proceedings of IEEE Aerospace Conference*, pages 1–9.

Huang, C., Qin, H., Zhao, C., and Liang, H. (2022). Phase - time method: Accurate Doppler measurement for Iridium NEXT signals. *IEEE Transactions on Aerospace and Electronic Systems*, 58(6):5954–5962.

Jardak, N. and Jault, Q. (2022). The potential of LEO satellite-based opportunistic navigation for high dynamic applications. *Sensors*, 22(7):2541–2565.

Jiang, M., Qin, H., Zhao, C., and Sun, G. (2022). LEO Doppler-aided GNSS position estimation. *GPS Solutions*, 26(1):1–18.

Kang, J., Eberechukwu N, P., Lee, J., Wymeersch, H., and Kim, S. S. (2024). Fundamental performance bounds for carrier phase positioning in LEO-PNT systems. In *Proceedings of IEEE International Conference on Acoustics, Speech and Signal Processing*, pages 13496–13500.

Kassas, Z. (2021). Position, navigation, and timing technologies in the 21st century. volume 2, chapter 43: Navigation from low Earth orbit – Part 2: models, implementation, and performance, pages 1381–1412. Wiley-IEEE.

Kassas, Z. and Humphreys, T. (2014). Observability analysis of collaborative opportunistic navigation with pseudorange measurements. *IEEE Transactions on Intelligent Transportation Systems*, 15(1):260–273.

Kassas, Z., Khairallah, N., and Kozhaya, S. (2024). Ad astra: Simultaneous tracking and navigation with megaconstellation LEO satellites. *IEEE Aerospace and Electronic Systems Magazine*, 39(9):46–71.

Kassas, Z., Kozhaya, S., Kanj, H., Saroufim, J., Hayek, S., Neinavaie, M., Khairallah, N., and Khalife, J. (2023). Navigation with multi-constellation LEO satellite signals of opportunity: Starlink, OneWeb, Orbcomm, and Iridium. In *Proceedings of IEEE/ION Position, Location, and Navigation Symposium*, pages 338–343.

Kelso, T. (2007). Validation of SGP4 and IS-GPS-200D against GPS precision ephemerides. In *Proceedings of AAS/AIAA Space Flight Mechanics Conference*, pages 1–14.

Kelso, T. (2022). NORAD two-line element set format. <https://celestrak.org/NORAD/documentation/tle-fmt.php>.

Khalife, J. and Kassas, Z. (2019). Receiver design for Doppler positioning with LEO satellites. In *Proceedings of IEEE International Conference on Acoustics, Speech and Signal Processing*, pages 5506–5510.

Khalife, J. and Kassas, Z. (2023). Performance-driven design of carrier phase differential navigation frameworks with mega-constellation LEO satellites. *IEEE Transactions on Aerospace and Electronic Systems*, 59(3):2947–2966.

Khalife, J., Neinavaie, M., and Kassas, Z. (2022). The first carrier phase tracking and positioning results with Starlink LEO satellite signals. *IEEE Transactions on Aerospace and Electronic Systems*, 56(2):1487–1491.

Kozhaya, S., Kanj, H., and Kassas, Z. (2023). Multi-constellation blind beacon estimation, Doppler tracking, and opportunistic positioning with OneWeb, Starlink, Iridium NEXT, and Orbcomm LEO satellites. In *Proceedings of IEEE/ION Position, Location, and Navigation Symposium*, pages 1184–1195.

Kozhaya, S. and Kassas, Z. (2023). Positioning with Starlink LEO satellites: A blind Doppler spectral approach. In *Proceedings of IEEE Vehicular Technology Conference*, pages 1–5.

Kozhaya, S. and Kassas, Z. (2024). A first look at the OneWeb LEO constellation: beacons, beams, and positioning. *IEEE Transactions on Aerospace and Electronic Systems*. accepted.

Kozhaya, S., Saroufim, J., and Kassas, Z. (2024). Starlink for PNT: a trick or a treat? In *Proceedings of ION GNSS+ Conference*. accepted.

Landry, R., Nguyen, A., Rasaee, H., Amrhar, A., Fang, X., and Benzerrouk, H. (2019). Iridium Next LEO satellites as an alternative PNT in GNSS denied environments—part 1. *Inside GNSS Magazine*, 14(3):56–64.

Leng, M., Qutin, F., Tay, W., Cheng, C., Razul, S., and See, C. (2016). Anchor-aided joint localization and synchronization using SOOP: Theory and experiments. *IEEE Transactions on Wireless Communications*, 15(11):7670–7685.

Li, M., Xu, T., Guan, M., Gao, F., and Jiang, N. (2022). LEO-constellation-augmented multi-GNSS real-time PPP for rapid re-convergence in harsh environments. *GPS Solutions*, 26(1):1–12.

Li, X. and Jilkov, V. (2003). Survey of maneuvering target tracking. Part I: Dynamic models. *IEEE Transactions on Aerospace and Electronic Systems*, 39(4):1333–1364.

Menzione, F. and Paonni, M. (2023). LEO-PNT mega-constellations: a new design driver for the next generation MEO GNSS space service volume and spaceborne receivers. In *Proceedings of IEEE/ION Position, Location, and Navigation Symposium*, pages 1196–1207.

Nardin, A., Dovis, F., and Fraire, J. (2021). Empowering the tracking performance of LEO-based positioning by means of meta-signals. *IEEE Journal of Radio Frequency Identification*, 5(3):244–253.

Neinavaie, M., Khalife, J., and Kassas, Z. (2022). Acquisition, Doppler tracking, and positioning with Starlink LEO satellites: First results. *IEEE Transactions on Aerospace and Electronic Systems*, 58(3):2606–2610.

Orabi, M., Khalife, J., and Kassas, Z. (2021). Opportunistic navigation with Doppler measurements from Iridium Next and Orbcomm LEO satellites. In *Proceedings of IEEE Aerospace Conference*, pages 1–9.

Osoro, O. and Oughton, E. (2021). A techno-economic framework for satellite networks applied to low earth orbit constellations: Assessing Starlink, OneWeb and Kuiper. *IEEE Access*, 9:141611–141625.

Prol, F., Ferre, R., Saleem, Z., Välisuo, P., Pinell, C., Lohan, E., Elsanhoury, M., Elmusrati, M., Islam, S., Celikbilek, K., Selvan, K., Yliaho, J., Rutledge, K., Ojala, A., Ferranti, L., Praks, J., Bhuiyan, M., Kaasalainen, S., and Kuusniemi, H. (2022). Position, navigation, and timing (PNT) through low earth orbit (LEO) satellites: A survey on current status, challenges, and opportunities. *IEEE Access*, 10:83971–84002.

Psiaki, M. (2021). Navigation using carrier Doppler shift from a LEO constellation: TRANSIT on asteroids. *NAVIGATION, Journal of the Institute of Navigation*, 68(3):621–641.

Reid, T., Chan, B., Goel, A., Gunning, K., Manning, B., Martin, J., Neish, A., Perkins, A., and Tarantino, P. (2020). Satellite navigation for the age of autonomy. In *Proceedings of IEEE/ION Position, Location and Navigation Symposium*, pages 342–352.

Reid, T., Walter, T., Enge, P., Lawrence, D., Cobb, H., Gutt, G., O’Conner, M., and Whelan, D. (2021). Position, navigation, and timing technologies in the 21st century. volume 2, chapter 43: Navigation from low Earth orbit – Part 1: concept, current capability, and future promise, pages 1359–1379. Wiley-IEEE.

Ries, L., Limon, M., Grec, F., Anghileri, M., Prieto-Cerdeira, R., Abel, F., Miguez, J., Perello-Gisbert, J., d’Addio, S., R. Ioannidis and, A. O., Rapisarda, M., Sarnadas, R., and Testani, P. (2023). LEO-PNT for augmenting Europe’s space-based PNT capabilities. In *Proceedings of IEEE/ION Position, Location, and Navigation Symposium*, pages 329–337.

Sabbagh, R. and Kassas, Z. (2023). Observability analysis of receiver localization via pseudorange measurements from a single LEO satellite. *IEEE Control Systems Letters*, 7(3):571–576.

Saroufim, J., Hayek, S., and Kassas, Z. (2023). Simultaneous LEO satellite tracking and differential LEO-aided IMU navigation. In *Proceedings of IEEE/ION Position Location and Navigation Symposium*, pages 179–188.

Saroufim, J., Hayek, S., and Kassas, Z. (2024). Analysis of satellite ephemeris error in differential and non-differential navigation with LEO satellites. In *Proceedings of IEEE Aerospace Conference*, pages 1–9.

Shahcheraghi, S. and Kassas, Z. (2024). A computationally efficient approach for acquisition and Doppler tracking for PNT with LEO megaconstellations. *IEEE Signal Processing Letters*, 31:2400–2404.

Stock, W., Schwarz, R., Hofmann, C., and Knopp, A. (2024). Survey on opportunistic PNT with signals from LEO communication satellites. *IEEE Communications Surveys & Tutorials*, pages 1–31. accepted.

Tan, Z., Qin, H., Cong, L., and Zhao, C. (2019a). New method for positioning using IRIDIUM satellite signals of opportunity. *IEEE Access*, 7:83412–83423.

Tan, Z., Qin, H., Cong, L., and Zhao, C. (2019b). Positioning using IRIDIUM satellite signals of opportunity in weak signal environment. *Electronics*, 9(1):37.

Thompson, S., Martin, S., and Bevly, D. (2020). Single differenced Doppler positioning with low Earth orbit signals of opportunity and angle of arrival estimation. In *Proceedings of ION International Technical Meeting*, pages 497–509.

Vallado, D. and Crawford, P. (2008). SGP4 orbit determination. In *Proceedings of AIAA/AAS Astrodynamics Specialist Conference and Exhibit*, pages 6770–6799.

Vetter, J. (2007). Fifty years of orbit determination: Development of modern astrodynamics methods. *Johns Hopkins APL Technical Digest*, 27(3):239–252.

Wang, K. and El-Mowafy, A. (2022). LEO satellite clock analysis and prediction for positioning applications. *Geo-spatial Information Science*, 25(1):14–33.

Wei, Q., Chen, X., and Zhan, Y. (2020). Exploring implicit pilots for precise estimation of LEO satellite downlink Doppler frequency. *IEEE Communications Letters*, 24(10):2270–2274.

Xie, Y., Li, G., Qin, H., Zhao, C., Chen, M., and Zhou, W. (2024). Carrier phase tracking and positioning algorithm with additional system parameters based on Orbcomm signals. *GPS Solutions*, 28(4):1–17.

Yan, T., Wang, Y., Li, T., Tian, Y., Qu, B., and Bian, L. (2023). MCSK signal for LEO satellite constellation based navigation augmentation system. In *Proceedings of China Satellite Navigation Conference*, pages 295–304.

Zhao, C., Qin, H., and Li, Z. (2022). Doppler measurements from multiconstellations in opportunistic navigation. *IEEE Transactions on Instrumentation and Measurement*, 71:1–9.

Zhao, C., Qin, H., Wu, N., and Wang, D. (2023). Analysis of baseline impact on differential Doppler positioning and performance improvement method for LEO opportunistic navigation. *IEEE Transactions on Instrumentation and Measurement*, 72:1–10.